ANAS Transactions **Earth Sciences** **1 / 2022**

http://www.journalesgia.com

HYDRO-GEOPHYSICAL PARAMETERS ESTIMATION OF POROUS AQUIFER USING GEOELECTRICAL TECHNIQUE-CASE STUDY FROM BAIJI–TIKRIT SUB-BASIN, IRAQ

Abdulrazzaq Z.T.[1], Ahmed M.M.[2], Salih S.A.[2], Asfahani J.[3]

[1] Directorate of Space and Communications, Ministry of Science and Technology, Baghdad, Iraq, 10070: zaidoon.taha@live.com

[2]Department of Applied Geology, College of Science, University of Tikrit, Tikrit, Iraq, 34001: dr.muhana@tu.edu.iq (M.M.A), sabbar.saleh@tu.edu.iq (S.A.S)

[3]Geology Department, Atomic Energy Commission, Damascus, Syria, P.O. Box 6091: jasfahani@aec.org.sy

Keywords: *VES, manual inverse modeling, hydro-geological characters, transmissivity, Baiji–Tikrit sub-basin, Iraq*

Summary. A geoelectrical survey is carried out in Baiji–Tikrit Sub-basin, Iraq, by applying the vertical electrical sounding (VES) technique to determine the thickness, extension, and hydraulic parameters of the main aquifers. A total of 40 VESs distributed along six geoelectrical profiles were executed using liner Schlumberger configuration, with a maximum half spacing of 400 m (AB/2 = 400 m), where a penetration depth of 151 m was reached. The VEWs curves are processed and interpreted manually by the auxiliary point method and automatically by IPI2win software using the manual inverse modeling to reduce the root mean square error ratio and increase the accuracy of the interpretation. The inversion results showed that the thickness of the main aquifer is about 50-128 m. The results of interpretation were used to draw a six geoelectrical sections along the survey traverses. Likewise, the results showed that the main aquifer of the area consists of sediments (sand, clay sand and clay) which belong to the Injana formation, whose conditions are apt to change in the area, from the confined type to the semi confined. Specific empirical relations have been established between the geoelectrical and hydraulic parameters. They are used to calculate the hydraulic conductivity (K) and the transmissivity (T) of the mean aquifer in the study area. The resulting K and T values are used to follow their spatial variations to delineate the suitable areas for new locations of wells.

1. Introduction

Water is an important component in several aspects of social life. Meanwhile, the drop in surface water makes the groundwater an excellent and essential resource for offsetting natural water shortages in places where surface water is scarce (Abdulrazzaq et al., 2020a; Gaikwad et al., 2021). The groundwater is considered one of the main national treasures; it is also considered an important parameter facing the shortage of surface water. To invest the groundwater properly, to lay down a model plan for wells distribution and to control the pumping operation, a hydrogeological evaluation system and hydraulic parameters of this aquifer will be needed (Kosinski and Kelly, 1981).

In contrast, random drilling can lead to drilling unproduced or little producing wells and/or may have a weak hydraulic property. It should therefore start with a geophysical survey in such kinds of studies before drilling to detect the depth, the thickness of underground (subsurface) aquifers, their water quality, and hydraulic parameters (Youssef, 2020; Abdulrazzaq et al., 2020b). There were a lot of geophysical methods to be used in such studies, but the famous and often one is the electrical resistivity (Keller, 1967; Soomro et al., 2019; Oudeika et al., 2021). The electrical resistivity technique is very popular due to its low cost, ease of application, and getting a fast result in comparison with the other methods (Lech et al., 2020; Virupaksha and Lokesh, 2021; AL-Awsi and Abdulrazzaq, 2022). Vertical Electrical Sounding (VES) is considered an essential geoelectrical technique that is widely used in groundwater investigation and deals with many problems in the subsurface layers (Agbasi et al., 2019; de Almeida et al., 2021).

Depending on the VES measurements, pumping test of the previous studies on some existing wells in the region, the aim of this study research can be concluded as the following:

- Estimating of the thickness and extension of the water-bearing beds.
- Delineating the groundwater system and water levels.
- Localizing the promising area and the candidate area of an expansion plan to drill a borehole for groundwater investment.

2. The study area

The study area is located between Tikrit and Baiji towns, on the western side of Tigris River, between longitudes 43º 56' 22.6"- 43º 40' 12.3" and latitude 34º 35' 13.3"- 34º 54' 41.7". It is bordered by the Tigris River from the east, subsurface Tikrit anticline from the west, Wadi Shishen from the south, and fields of sand dunes from the north and northwest of the area (Fig.1). The area was semi-rectangular shape of 45 km length, and 700 km^2 of total area.

The age of the exposed rocks was ranged from the Middle Miocene to the Quaternary, Injana formation, the oldest one was exposed in the northern part of the region (Fig.2), and in Wadi Shishen (southern part). It is composed of alternation of fractured claystone, siltstone and sandstone (Hamza et al., 1990).

The Quaternary deposits were divided into two parts, firstly, the Pleistocene deposits composed of gravel (river terraces), besides the gypserious soil (Gypcrite). The size of these deposits is ranged from boulder to pebble, and they are weakly cemented, that led to be a good strata to penetrate the water to underground aquifers (Al-Ani, 1997). The deposits were divided into four facies, like clayey gravel, clayey sandy gravel, sandy gravel and sandy clayey gravel (Basi and Karim, 1990), while the gypsions soil covers a large part of the area and contains of gravel, sand, silt and clay, which were rich by secondary gypsum, classified as gypcrite facies (gypsious soil).

The Holocene deposits consist of soft detroital deposits, like flood plain of the Tigris River between Baiji and Tikrit in a zigzag belt of 3 km width, and more than 3 meters thickness sediments alternation of sand, silt and clay silt, valley deposits of gravel, sand, silt, clay and gypsum, which came from the surrounding high areas (Al-Janabi, 2008). Sand dunes deposits are also existed in NW part of Baiji, making a recent cover over sediments (Jassim and Goff, 2006). Geomorphologically the area is a plain shape in general, with small valleys directed to east and southeast towards the Tigris River. The river terraces cover 2/3 of the region with gypseous soil and gravel. The area is elevated between 160 m above sea level on the western part near Tikrit anticline and 100 m towards the Tigris River on the east. The seasonal valleys are the most observed geomorphologic features, characterized by the two systems, dendritic and parallel valleys. These valleys are concentrated to the western part, near the subsurface Tikrit anticline (Fig. 2) to form the surface discharge system, which diverted to the southeast to be ended at the Tigris River via the Wadi Shishen valley. In general, the valleys are gently sloped, filled by loose fine grains sediments.

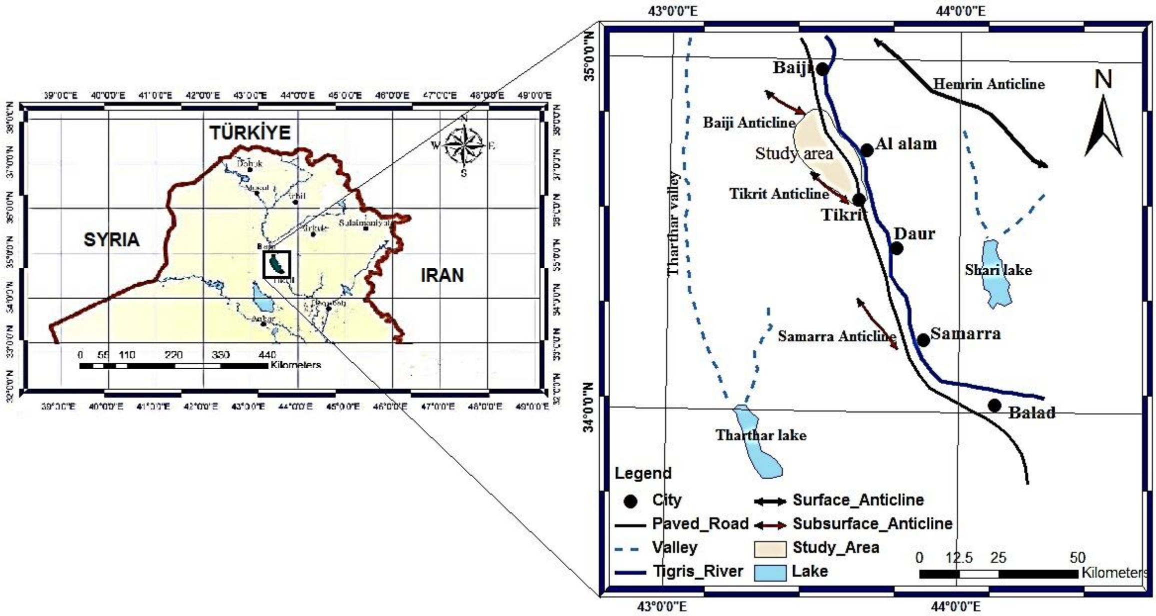

Fig. 1. Location map of the study area

The north–northwest part of the region is characterized by less dominant valleys that ended with depressions inside the study area to capture the rainwater to recharge the underground aquifers (Abdulrazzaq, 2011). While the eastern part of the study area, which runs parallel to the Tigris River, consists of a group of short valleys that started from the edge of river terraces and finished east toward the river. Other geomorphological features are existed, like the scarps, falling mass accompany in the Tigris River, and the existence of dunes and sand sheets (Al-Ani, 1997).

Tectonically the area lies within the Mesopotamian zone, Ammara–Tikrit secondary subzone (Al-Kadhimi et al., 1996), and belongs to the unstable shelf, according to (Buday and Jassim, 1984). There are no surface features that can indicate the structural phenomena, except the existence of the NW-SE Tikrit subsurface anticline, along the western side of the area. This subsurface structure affected the topography, and there is also a fault intersecting the Tikrit structure. This deep-seated fault has extended from the Jurassic till Miocene rock (Al-Kadhimi et al., 1996; Hamza et al., 1990; Al-Ani, 1997). It is believed that there are many subsurface faults in the region, which had a significant effect on the aquifer properties because, they are changing from confine to semi and unconfined types due to the hydraulic connection resulting from the fracturing of faults.

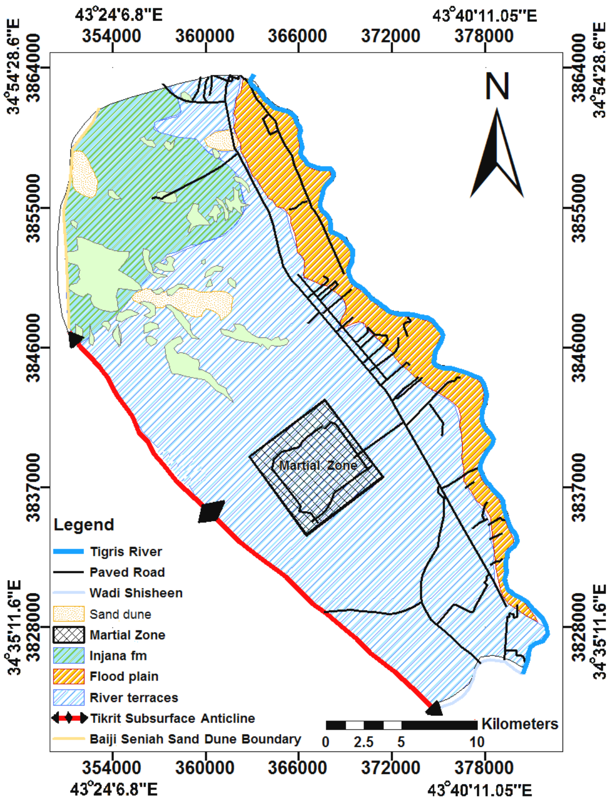

Fig. 2. Geological map of the study area

3. Materials and Methods

3.1. Data Acquisition

French Syscal R2 resistivity meter, IRIS, was used to measure forty VES points with asymmetrical Schlumberger arrangement. Those VES points are distributed along with six profiles of 6-14 km length (Fig.3). Fife of them are oriented NE-SW, perpendicular to the subsurface anticline axis existing in the area of NW-SE direction. At the same time, the sixth geoelectric profile (H'-H) was directed to be perpendicular to the other profiles (C'-C, D'-D, F'-F) and parallel to the subsurface strike, to illustrate the aquifers expansion in this direction. A significant effect of the existing structures in the study area is evident on the groundwater aquifers, which control the hydraulic parameters (Al-Kadhimi et al., 1996; Hamza et al., 1990).

The distance between the profiles is 4.6 km, with a 2 km offset between two successive VES points. The direction of electrode layout for the measured VES points was oriented to be parallel to beds strike (i.e., NW-SE) to illuminate the strata-dip effect. GPS was also used to get the elevation and attitude of the measured VES points.

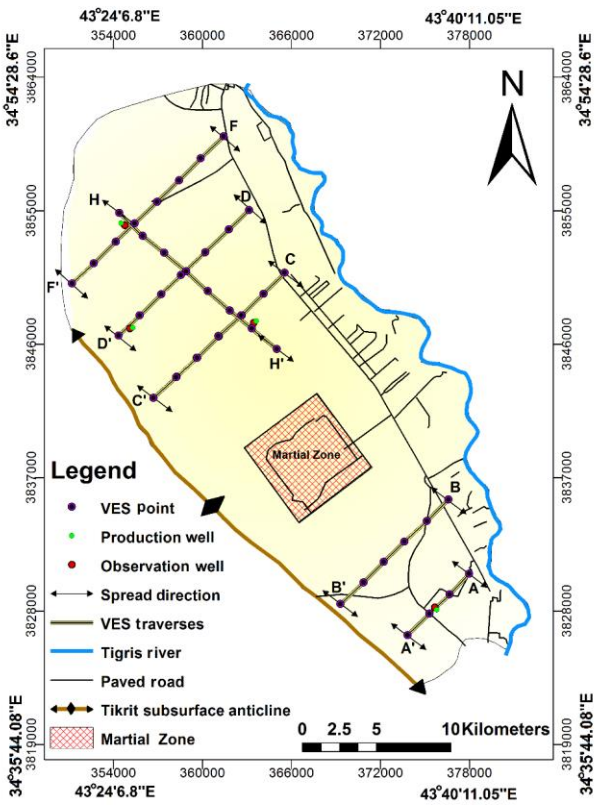

Fig. 3. Location of VES points, the direction of profiles, and electrode layout orientation

3.2. Vertical Electrical Soundings (VES)

The VES technique is generally used to determine the vertical variations in electrical resistivity. In this technique, an electrical current was imposed on the study area by a pair of electrodes A and B at varying spacing, expanding symmetrically from a central point while measuring the surface expression of the resulting potential field with an additional pair of electrodes M and N at the appropriate spacing. For a given position A, B, M and N, the apparent resistivity (ρa) is expressed by the following equation:

$$\rho a = \frac{2\pi}{\frac{1}{AM} - \frac{1}{BM} - \frac{1}{AN} + \frac{1}{BN}} \frac{\Delta V}{I} \quad , \qquad (1)$$

where I is the current introduced into the earth, and ΔV is the potential measured between the potential electrodes.

The apparent resistivity values "ρa" are obtained by increasing the electrode spacing about a fixed point and plotted against half electrode separation (AB/2) to establish field resistivity curve as shown in Fig. 4.

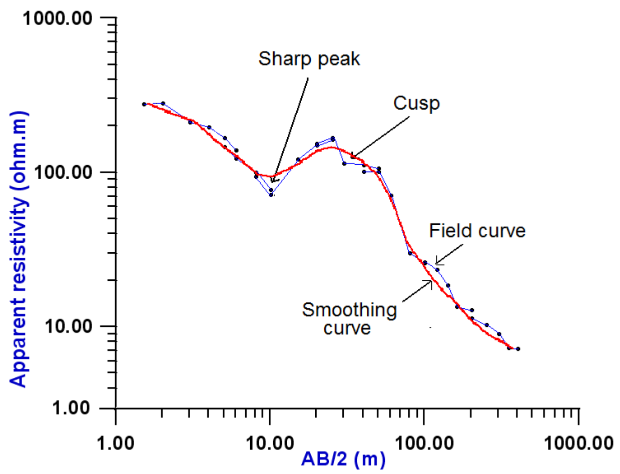

Fig. 4. Field VES sounding at point 3A

The curve matching technique using master curves (Orellana and Mooney, 1966) is firstly used to interpret the field resistivity curves to obtain the initial approximate model of thicknesses and resistivities of corresponding layers. The parameters of the approximate model, after that, are accurately interpreted with an inverse technique program until the goodness of fit between the field resistivity curve and the theoretical regenerated curve was reached (Zohdy, 1989; Zohdy and Bisdorf, 1990). The inversion software IPI2win has been used to interpret the VES soundings in terms of one dimension (1D) to get the final geoelectrical models for the interpreted VES soundings (Bobachev, 2002), as shown in Fig. 5.

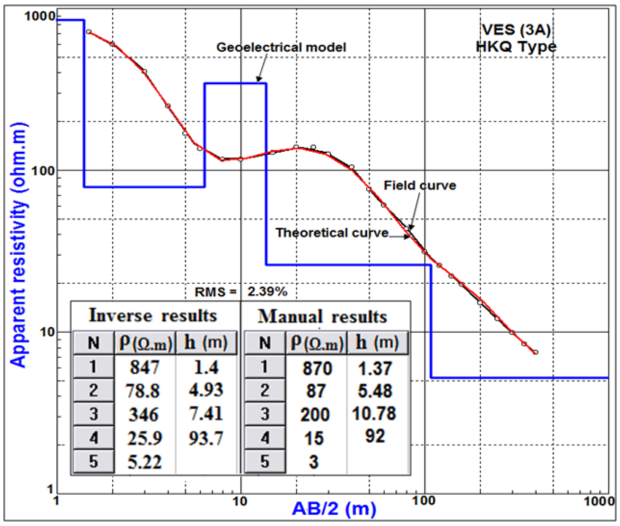

Fig. 5. The inversion model was obtained at VES point 3A

4. Results and Discussion

4.1. Geoelectrical and geological sections

The measured VES points are distributed along with six profiles (A-A', B-B', C-C', D-D', F-F', and H-H') (Fig.3). The description of those profiles are as follows:

1- The geoelectrical section along A-A' profile:

This profile passes through four VES points (Fig.6), and the VES sounding point (3A) was located near observation well 4 (Ob. well 4).

The conjoint correlation of the interpreted VES sounding points with the Ob. well 4 (Fig. 7) allows to assess the ranges of both resistivity and the equivalent thickness for the different following observed zones:

a- The first zone:

This zone is represented by topsoil, divided into two sub-zones; the first is the soil subzone of a high resistivity ranging between 292-882.3 Ω.m, its thickness ranges between 1.356-1.94 m. It is due to the soil moisture differences and discrepancy of properties. The second sub-zones have a low resistivity ranging between 68.7-98.5 Ω.m, and their thickness ranges between 4.9-8.4 m. The total thickness of the first zone therefore ranges between 6.33-9.76 m.

b- The second zone:

This zone consisting of coarse gravel deposits is represented by river terraces belonging to the Quaternary. Its resistivity ranges between 140-346 Ω.m, while its thickness is between 7.41-14.74 m.

c- The third zone:

This zone represents the unconfined aquifer due to the unseen existing confined layer bounded by the aquifer from the top. Therefore, lowered resistivity values 19.3-52.9 Ω.m are noticed.

This zone is characterized by a relatively high thickness ranging between 89.8 and 97.7 m. It consists of coarse gravel at the top, representing the river terraces of 26 m thickness. This was detected depending on the observation well 4. The middle and lower parts of this zone consist of sand, clay, and clay sandy deposits of the Injana formation.

The resistivity values increase at points 1A and 4A due to the decrease of porosity water salinity because the location of VES point 1A is near the Tigris River. The VES point 4A is characterized by high resistivity values due to the percolation of rainwater through the valleys located near the VES point 4A, where this point is approached from the recharge area of the aquifer represented by the subsurface anticline located west of the profile.

d- The fourth zone:

This zone is the last one and represents the lower boundary of the aquifer, and its resistivity values essentially decrease to reach an average value of 6.6 Ω.m.

This zone consists of claystone saturated with saline water (AL-Minshid, 2001). The claystone layer is not recognized in the drilled well section in the area because of the limited depth, while this same zone was observed at the same depth in the Al-Minshid study, 2001.

2- The geoelectrical section along B-B' profile

The B-B' profile passes through six VES sounding points (Fig. 8). A large similarity in terms of the number of zones and the resistivity values are found between this profile with that of profile A-A'.

3- The geoelectrical section along C-C' profile:

The C-C' profile passes through seven VES sounding points (Fig.9). A correlation process of VES point interpretation made with the stratigraphic section of observed well No.3 allows to define the different ranges of both resistivity and equivalent electrical zones.

4- The geoelectrical section along D-D' profile:

Fig.10 shows the location of seven VES points distributed on this D-D' profile.

The correlation is made between the interpreted VES point 7D and the stratigraphic section of observed well No.2, allowing defining the different ranges of both resistivity and equivalent electrical zones.

5- The geoelectrical section along F-F' profile:

This profile passes through eight VES points (Fig.11). The correlation of interpreted VES point 5F with the stratigraphic section of the observed well No.1 is carried out to define the different ranges of both resistivity and equivalent electrical zones.

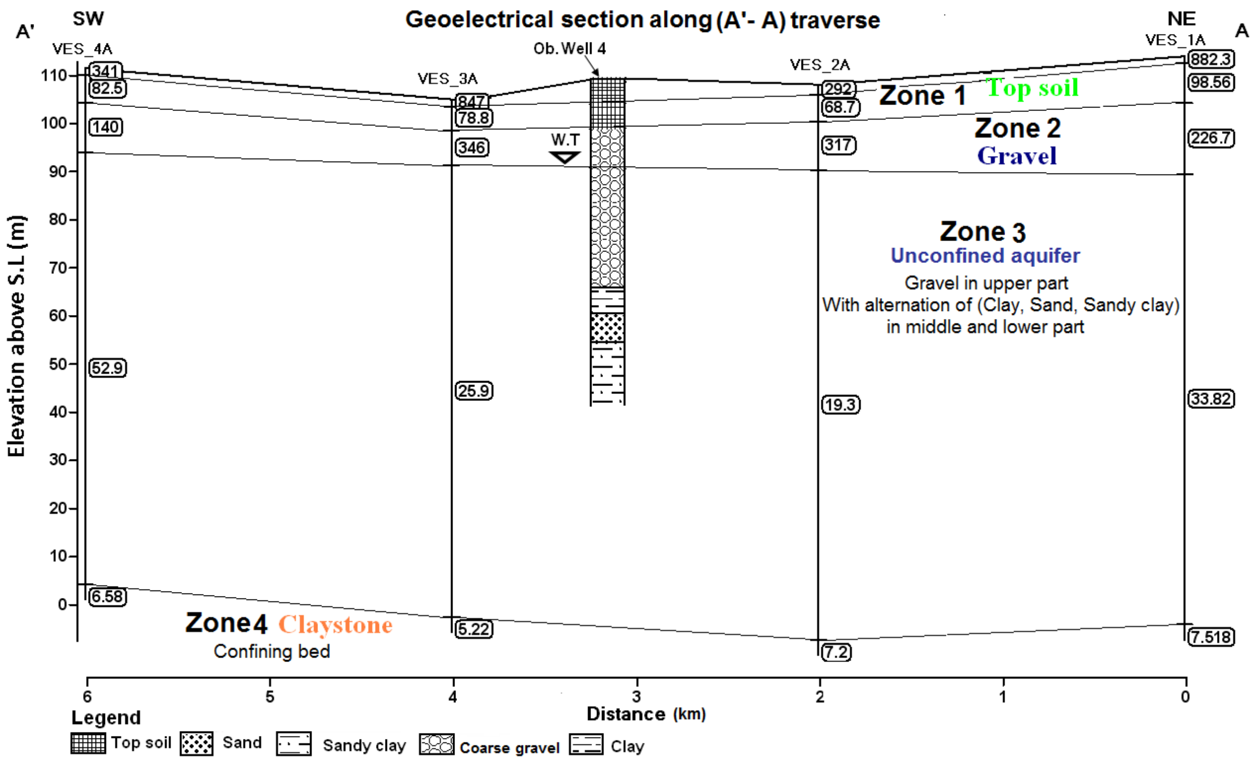

Fig. 6. The geoelectrical section along A-A' profile

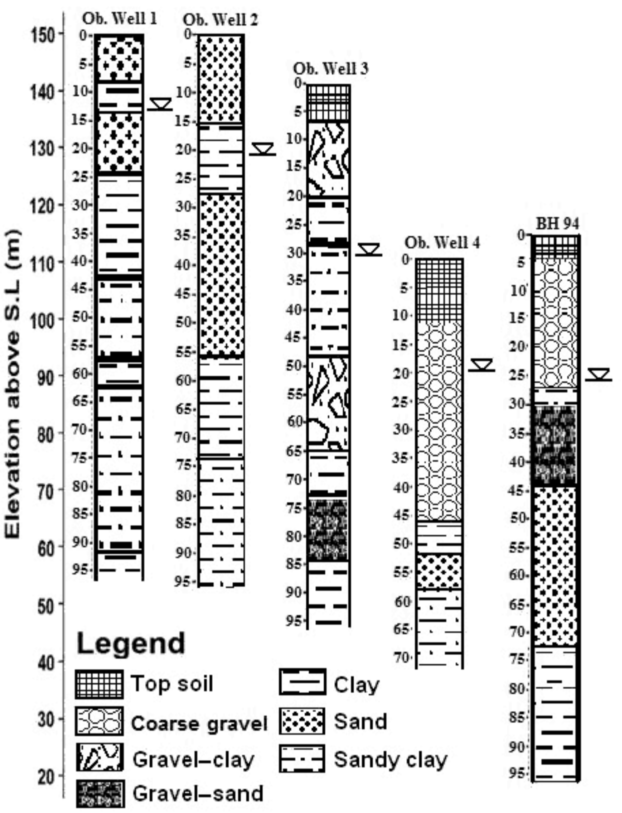

Fig. 7. The lithological description of the dried wells in the study area

6- The geoelectrical section along H-H' traverse:

The H-H' profile is located perpendicularly on the three previous C-C', D-D', and F-F' profiles and passes through eight VES points (Fig.12). The correlation of the interpreted VES points (1H, 7H) with the stratigraphic section of observed wells No. 1 and 3 are carried out to define the different ranges of both resistivity and equivalent electrical zones.

A regional fault plane passing through the study area and crossing the H-H' profile between the VES points 3H and 4H is located. This fault plays the primary role in controlling the factors of the aquifer parameter in the study area. The study of this profile reveals the presence of five different electrical zones, as shown in Fig.11.

4.2. Calculation of thickness and resistivity of aquifer

The use of the final 1D interpretation of vertical electrical sounding (VES) and the drilling wells information in the study area allow the thickness and resistivity values of the saturated aquifer to be known for all studied VES points. The spatial variations of the saturated thickness and resistivity maps of the aquifer are constructed as shown in Fig.13 and Fig.14. It is noticed from Fig.13 that aquifer saturated layer thickness is relatively constant at most of the studied area, except the northwest part, where an increased thickness towards the northwest of the study area up to 138 m is observed. This increment coincides well with the position of displacement caused by the subsurface fault indicated in the geoelectrical section along H-H' profile.

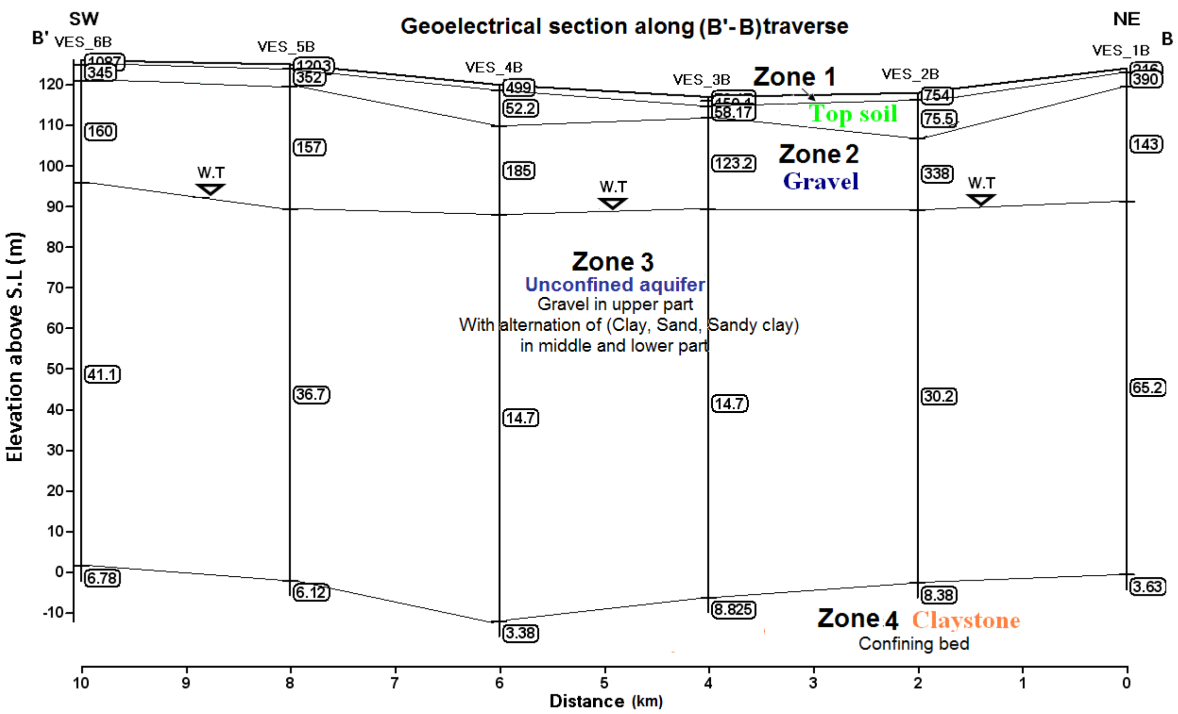

Fig. 8. The geoelectrical section along B-B' profile

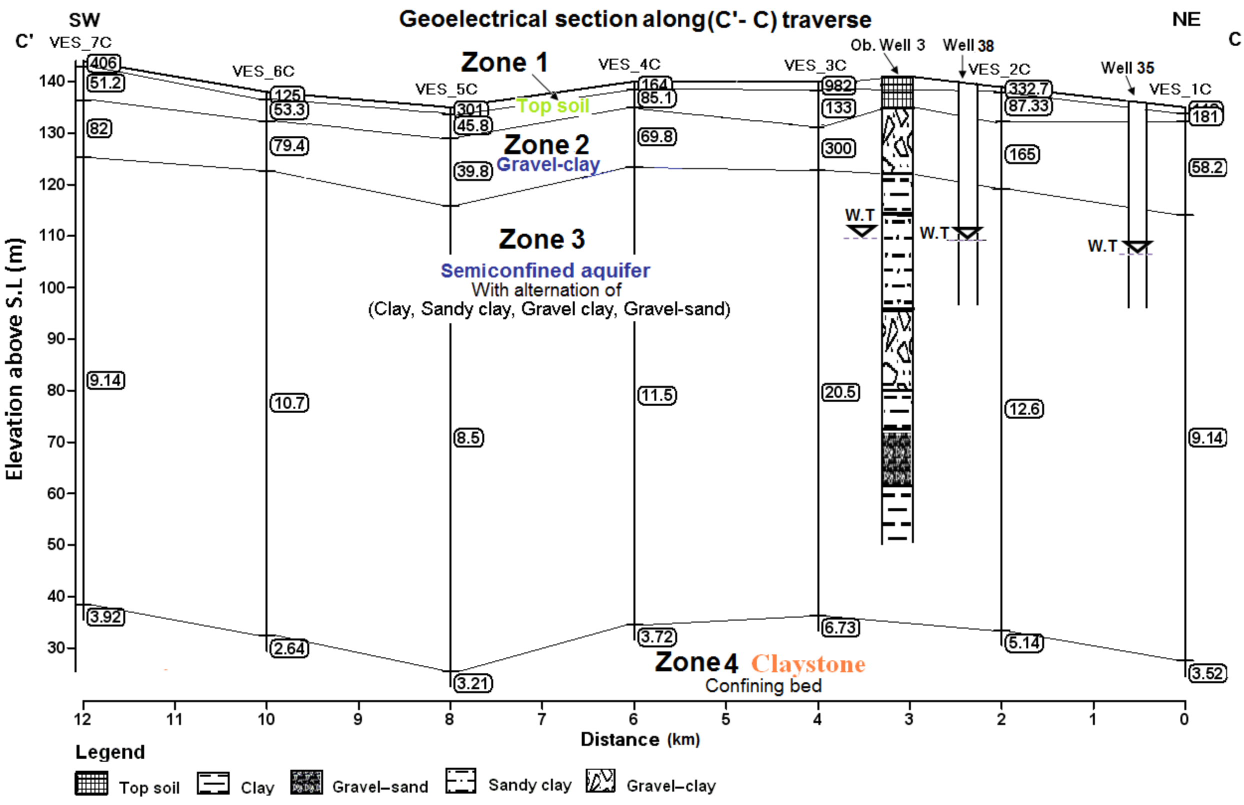

Fig. 9. The geoelectrical section along C-C' profile

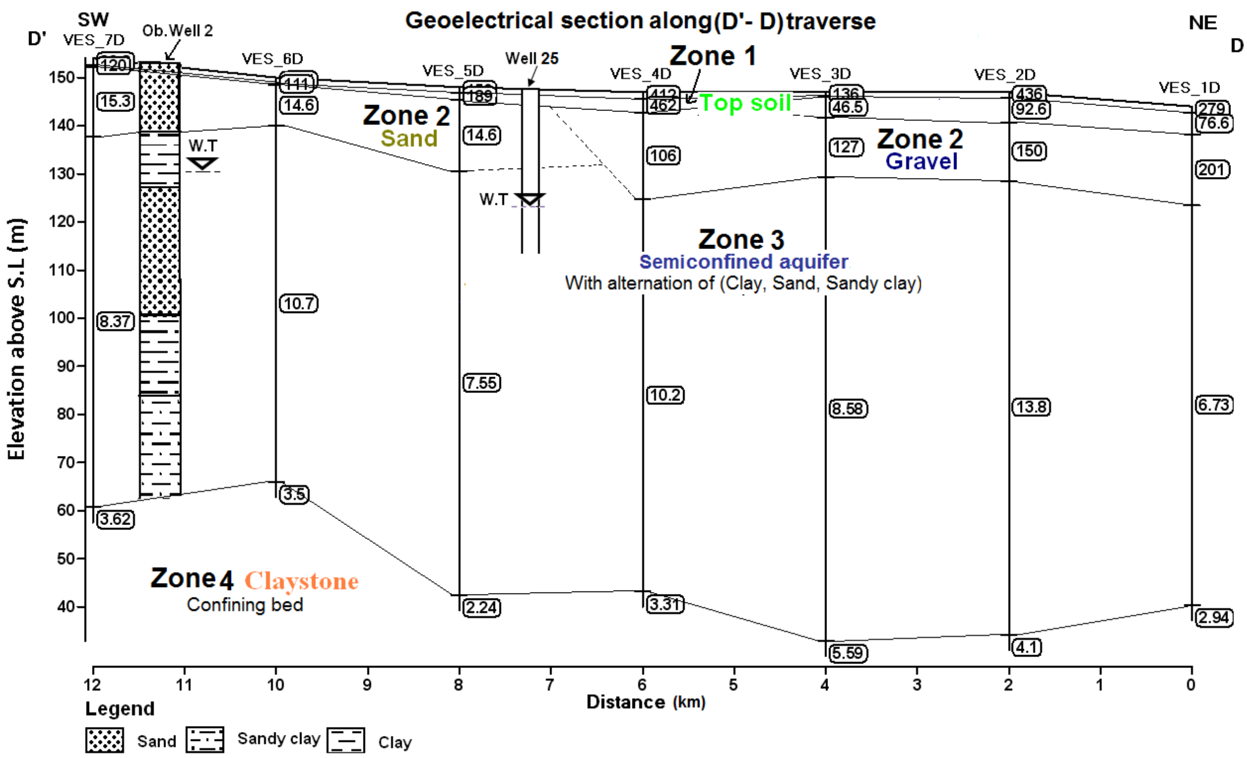

Fig. 10. The geoelectrical section along D-D' profile

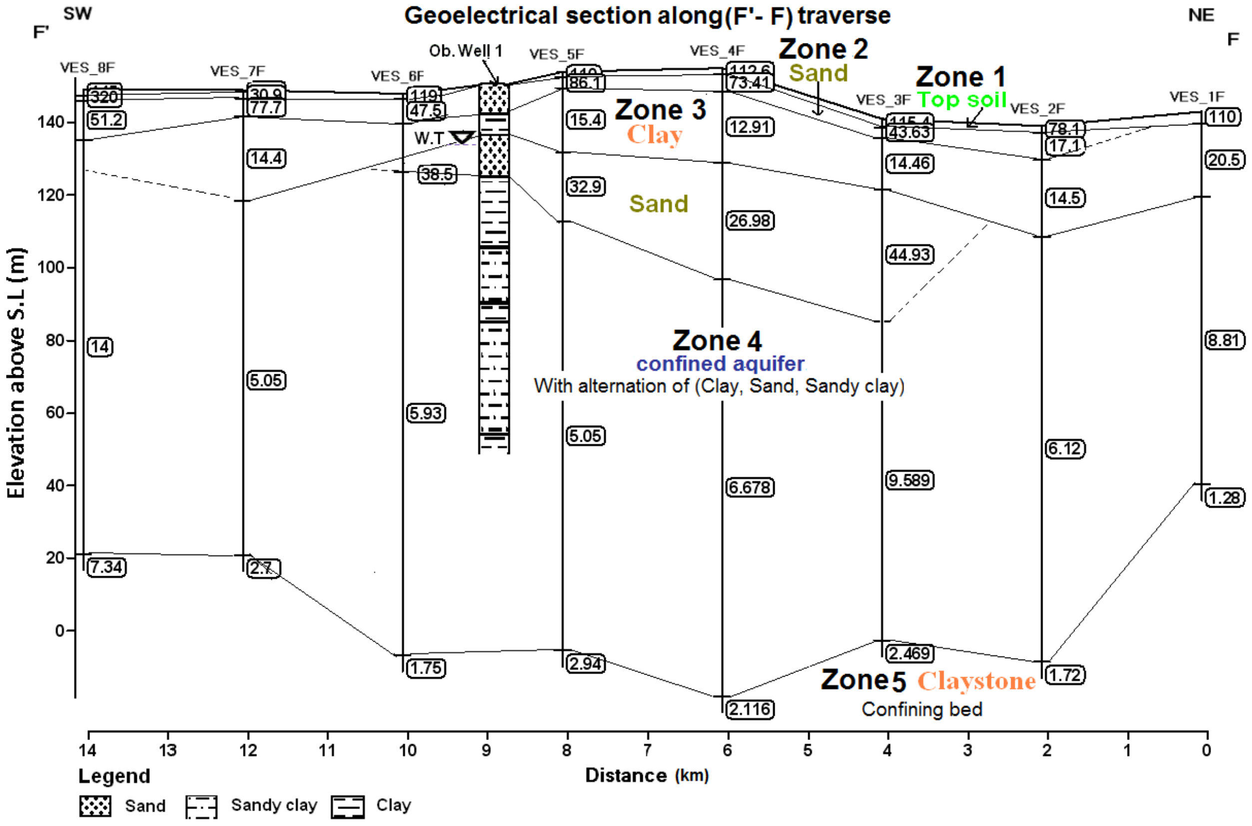

Fig.11. The geoelectrical section along F-F' profile

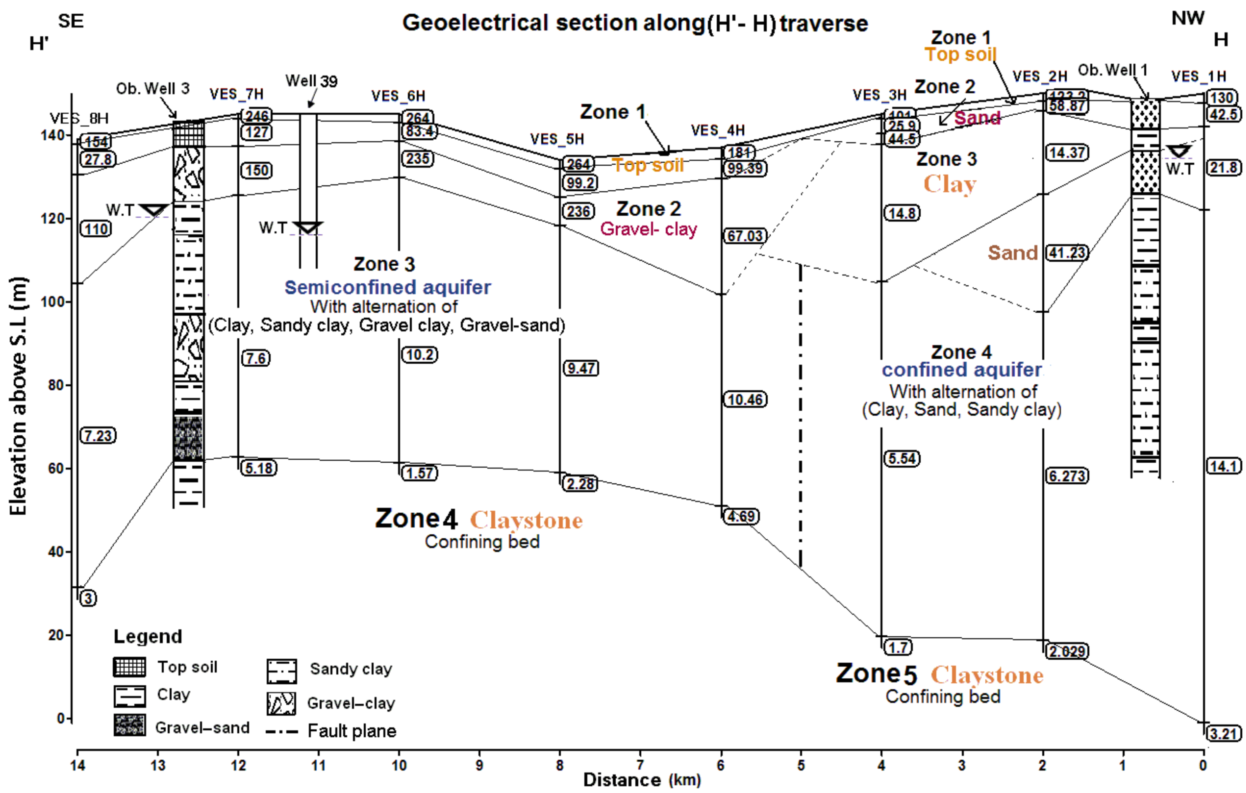

Fig. 12. The geoelectrical section along H-H' profile

The rest of the study area is characterized by a gradually gentle increase in the saturated zone thickness, starting from the area of the subsurface fault, towards the southeast of the area, the thickness of the zone is about 50-95 m. The reason for such increase is due to the increase of gravel layer thickness of the Quaternary deposits in this direction, near the Tigris river, to reach of about 40 m layer thick, which was considered in some areas, as a part of the aquifer in the region.

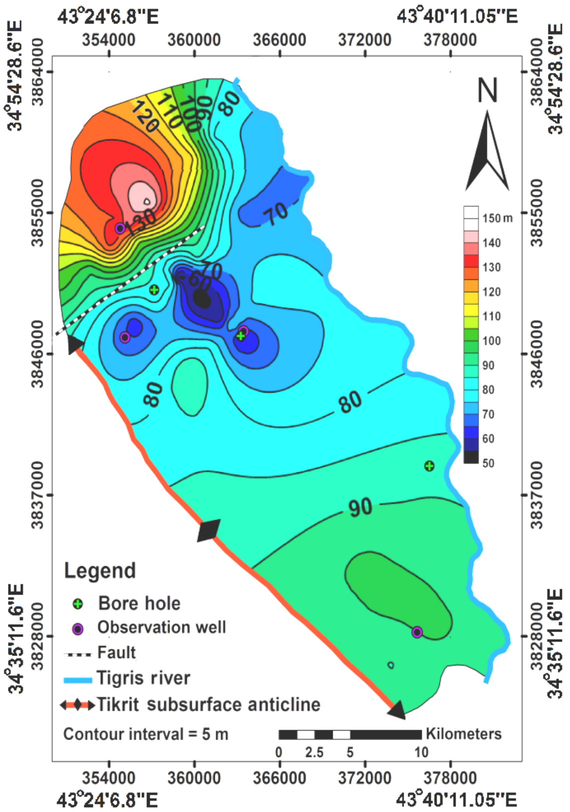

Fig. 13. Spatial variation map of the saturated layer thickness in the study area

The spatial variation map of the saturated layer shows an increase in resistivity values corresponding to the increase of the saturated zone thickness. The presence of the fault led to the depletion of the saline groundwater from lower aquifers, which in turn led to a decrease in the resistivity values in the northern region around the fault. However, the resistivity increases on both sides from the north due to the recharge area towards the subsurface anticline and from the right due to the interference of the freshwater of the Tigris River with the saline groundwater which in turn works to raise the values of the specific resistivity.

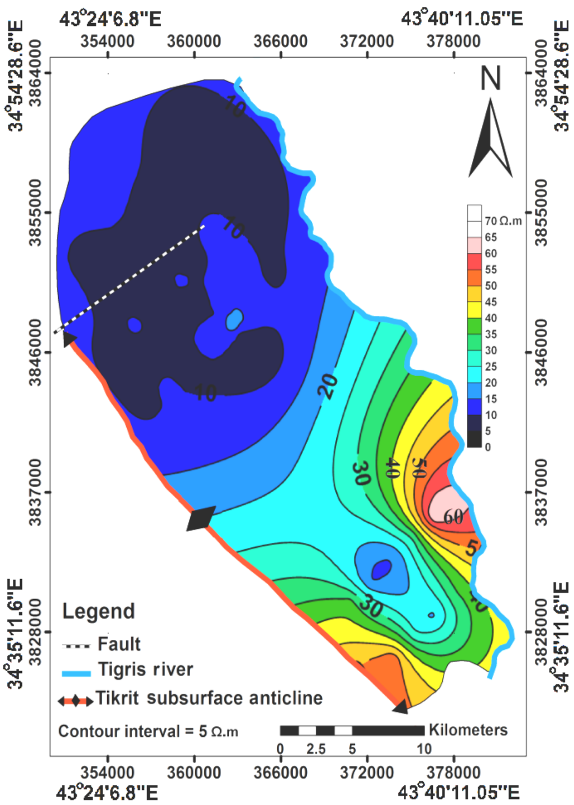

Fig. 14. Spatial variation map of the saturated layer resistivity in the study area

4.3. The geoelectrical and hydraulic parameters relations

The available geoelectrical and hydraulic parameters of four VES points (1D) curves interpretation, located about one km away from four observed wells in the study area aquifer, are conjointly used to get more precise empirical relations between them. The transmissivity values shown in Table 1 were obtained from the experiment pumping test results using Jackob's method, carried out by (Al-Jobori, 2011), for the mentioned four wells.

The hydraulic conductivity values were calculated from the relation between the transmissivity and the thickness of the aquifer.

Table shows the geoelectrical and hydraulic parameters for the aquifer for four VES points that we use to find some specific empirical relationship between them.

VES No.	Well No.	Aquifer thickness (m)	Aquifer resistivity ρ (ohm.m)	Transmissivity T (m²/day)		Hydraulic Conductivity K (m/day)		Profile resistivity ρ_t (ohm.m²)	Longitudinal conductance S (ohm⁻¹)
				Theis	Jacob	Theis	Jacob		
3A	Ob.4	93.7	25.9	881.9	838.2	16.64	15.82	2426.83	3.61
7D	Ob.2	70	8.37	162.1	197.7	2.15	2.63	585.9	8.36
1H	Ob.1	129	14.1	1092	820.9	13.24	9.95	1818.9	9.14
7H	Ob.3	57.27	7.6	152.2	233.3	2.34	3.58	435.25	7.53

4.4. The relation of geoelectrical parameters with transmissivity

The available data of four wells allow applying the regression analysis to find some empirical relationships as:

- Relation of aquifer resistivity (ρ) with hydraulic conductivity (K).
- Relation of transverse resistivity (ρt) with longitudinal electric conductivity (S).
- Relation of the transmissivity (T) with the transverse resistivity (ρt).
- Relation of the transmissivity (T) with the longitudinal electric conductivity (S).

The coefficient regression between aquifer resistivity and hydraulic conductivity is of R^2= 0.94 with the use of equation shown in Fig.15.

The equation shown in Fig.15 is therefore used to compute the hydraulic conductivity values at any location within the studied area by getting the aquifer resistivity at that location. The resulting hydraulic conductivity map is shown in Fig.16.

The regression relation between the transverse resistivity (ρt) and the transmissivity is shown in Fig. 17b and has R^2= 0.93. This means that the transverse resistivity controls and dominates well the study aquifer.

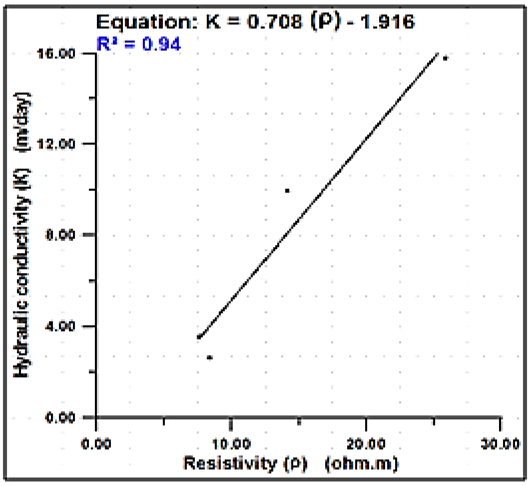

Fig. 15. The regression relation of the resistivity and hydraulic conductivity for the aquifer

The weak connection shown in Figs 17a, and 17c is due to the presence of clay ratio in the aquifer that causes the distortion in the longitudinal electric conductivity relation with both transverse resistivity and transmissivity. The equation shown in Fig.17b is therefore used to compute the transmissivity values at any location within the study area by getting the transverse resistivity at that location. The resulting transmissivity map (Fig.18) is used to delineate the high values, representing the locations of new suggested wells of good production. The transmissivity increases towards the south and southeast (Fig.18), where this increasing coincides well with the active porosity and thickness of the Quaternary gravel within the aquifer.

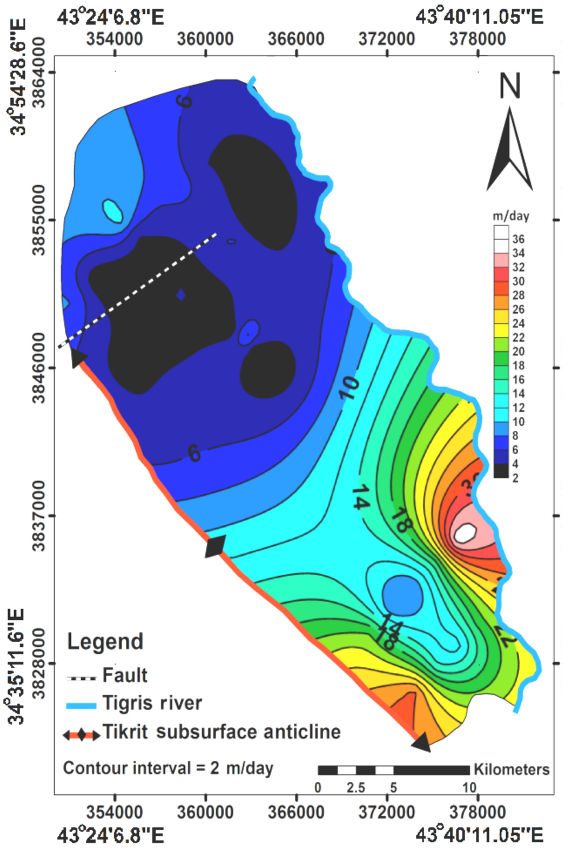

Fig. 16. Hydraulic conductivity map of the study area, according to geoelectrical properties

5. Conclusions

Depending on the quantitative result interpretation of the VES points, on the geological-hydrogeological information, and the suggested geophysical model, we can conclude as follows:

1- Two aquifers were detected in the region, these are:

a- The primary main aquifer is represented by the Injana formation (U-Miocene) (sand, clay sand, and clay). This aquifer changes its type from the confining aquifer one, in the northern part of the region, to the semi-confine aquifer in the mid- and south of the region. This aquifer has a thickness ranging of 50-128m, increasing in the northern part due to the displacement of the regional fault. On the other hand, the thickness of the aquifer was relatively constant in the middle and southern regions.

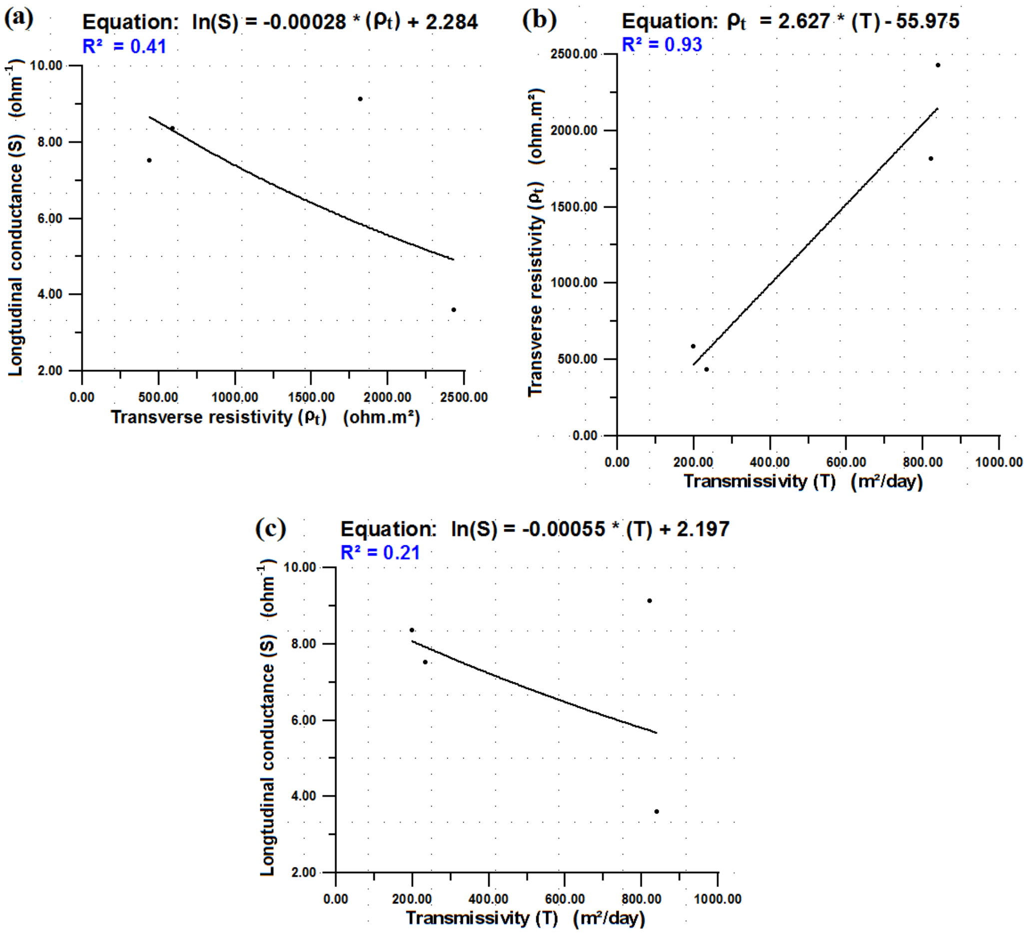

Fig. 17. Three experimental relationships for the study aquifer between a: profile resistivity – longitudinal conductance; b: transmissivity – profile resistivity; c: transmissivity – longitudinal conductance

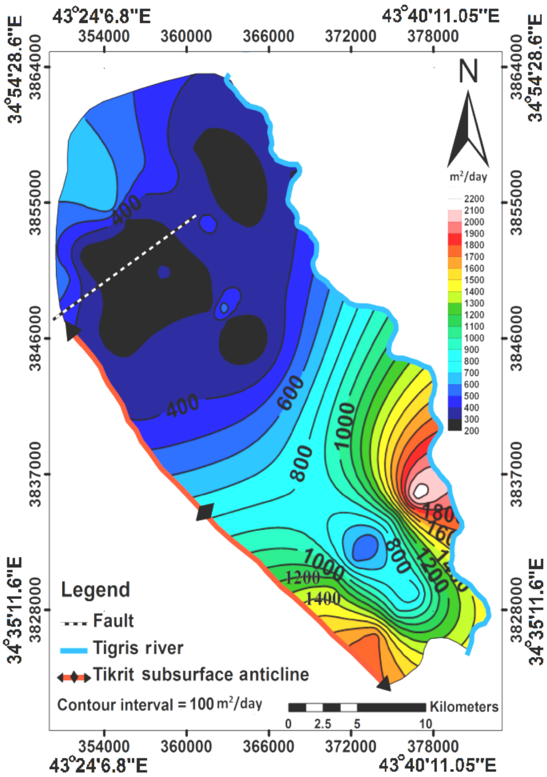

Fig. 18. Transmissivity map of the study area, according to geo-electrical properties

b- Secondary unconfined aquifer that consists of gravels of river terraces of the Quaternary appears in the southern part of the region at the Traverses A-A', B-B' only, and exists at the top of the main aquifer with 5-25 m thickness. Its resistivity changes from 39.8 to 346 Ωm due to the existent lateral and vertical changes of clay – secondary gypsum ration.

2- The clay layer, as the lower boundary of the main aquifer, has a very low resistivity ranging between 1.28-8.3 Ωm, which helps to delineate the depth penetration of the survey. These low resistivity layers could be saturated salted groundwater (due to the concentration of the current in this layer).

3- Groundwater table ranged between 87.97 to 130.87 m, above sea level, which increases in the northern part of the region as approached from the subsurface fold, while decreases in the middle and southern part of the region, i.e., towards the discharge area (River).

4- The computed transmissivity values of the aquifer range between 200-2200 m^2/day, while the values of hydraulic conductivity range between 2-36 m/day. These variations were due to the following:

a- Increasing and decreasing of the saturated thickness: profile resistivity was usually proportional with thickness, hydraulic conductivity, and transmissivity.

b- Lithological variety: Aquifer resistivity was proportional to the profile resistivity and changing active porosity, affecting the hydraulic conductivity.

c- Clay ratio: increasing the clay ratio leads to a decrease in the profile resistivity value and active porosity, which are both proportional with the transmissivity and the hydraulic conductivity.

5- VES points along traverses A-A' and B-B' could be considered as new locations for very high production wells due to their high values of transmissivity, ranging between 552.9-2180 m^2/day and high thickness of the aquifer ranged between 89.9-100 m. As well as the VES points (3C, 2D, 3F, 4F, 1H), which have a transmissivity value of 403, 547, 700, 612, 445 respectively.

6- Many quarries can be located to exploit the Quaternary gravel in the south of the area, as approaching the river.

Acknowledgment

The researchers are grateful to the general directory of groundwater for their help in getting the data, and special thanks go to messeiers: Ahmed Sardah Alzubaidy, Dhia Besho, and Sherif Reshad, Ahmed Al-dory of the Salah El-Din branch of the directory of groundwater. Thanks to Prof. Dr. Jassim Thabit for his help in data interpretation and criticism.

REFERENCES

Abdulrazzaq Z.T. Application of vertical electrical sounding to delineate and evaluate of aquifers characteristics in Baiji-Tikrit Basin. M.Sc. Thesis, University of Tikrit, 2011,10 p.

Abdulrazzaq Z.T., Agbasi O.E., Aziz N.A., Etuk S.E. Identification of potential groundwater locations using geophysical data and fuzzy gamma operator model in Imo, Southeastern Nigeria. Applied Water Science, Vol. 10, No. 8, 2020a, 188, https://doi.org/10.1007/s13201-020-01264-6.

Abdulrazzaq Z.T., Al-Ansari N., Aziz N.A., Agbasi O.E., Etuk S.E. Estimation of main aquifer parameters using geoelectric measurements to select the suitable wells locations in Bahr Al-Najaf depression, Iraq. Groundwater for Sustainable Development, Vol. 11, 2020b, 100437, https://doi.org/ 10.1016/j.gsd.2020.100437.

Agbasi O.E., Aziz N.A., Abdulrazzaq Z.T., Etuk S. E. Integrated geophysical data and GIS technique to forecast the potential groundwater locations in part of South Eastern Nigeria. Iraqi Journal of Science, Vol. 60, No. 5, 2019, pp. 1013-1022.

Al-Ani A.A. The optimum investment of groundwater in Fatha-Samarra basin. M.Sc. thesis, college of science, University of Baghdad, 1997, 114 p.

AL-Awsi M.H. and Abdulrazzaq Z.T. Implementing electrical resistivity tomography to delineate soil contamination zone, Southern Baqubah City, Iraq. Kuwait Journal of Science, Vol. 49, No. 2, 2022, https://doi.org/10.48129/kjs.10674.

Al-Janabi M.A.J. Hydrochemistry of the unconfined aquifer and the relationship of unsaturated zone sediments on the groundwater quality in Tikrit – Samara basin, Ph.D. thesis, college of science, University of Baghdad, 2008, 154 p.

Al-Jobori N.H. Hydrogeological conditions of Baiji-Tikrit sub basin, M.Sc. thesis, college of science, University of Tikrit, 2011, 164 p.

Al-Kadhimi J.A.M., Sissakian V.K., Satter A.F., Diekran D.B. Tectonic map of Iraq, Scale 1:1,000,000. 2nd Edition, GEOSURV, Baghdad, 1996.

Al-Minshid F.H.K. Groundwater study of Al-Dhibaee area using electrical survey and pumping test wells. M.Sc. thesis, college of science, University of Baghdad, 2001, 119 p.

Basi M.A. and Karim S.A. The stage report of the local geological survey, Vol. 2, 1990, Laboratory Studies.

Bobachev C. "IPI2Win": a Windows software for an automatic interpretation of resistivity sounding data. PhD tesis, Moscow State University, Moscow, Russia, 2002, 320 p.

ЛИТЕРАТУРА

Abdulrazzaq Z.T. Application of vertical electrical sounding to delineate and evaluate of aquifers characteristics in Baiji-Tikrit Basin. M.Sc. Thesis, University of Tikrit, 2011,10 p.

Abdulrazzaq Z.T., Agbasi O.E., Aziz N.A., Etuk S.E. Identification of potential groundwater locations using geophysical data and fuzzy gamma operator model in Imo, Southeastern Nigeria. Applied Water Science, Vol. 10, No. 8, 2020a, 188, https://doi.org/10.1007/s13201-020-01264-6.

Abdulrazzaq Z.T., Al-Ansari N., Aziz N.A., Agbasi O.E., Etuk S.E. Estimation of main aquifer parameters using geoelectric measurements to select the suitable wells locations in Bahr Al-Najaf depression, Iraq. Groundwater for Sustainable Development, Vol. 11, 2020b, 100437, https://doi.org/ 10.1016/j.gsd.2020.100437.

Agbasi O.E., Aziz N.A., Abdulrazzaq Z.T., Etuk S. E. Integrated geophysical data and GIS technique to forecast the potential groundwater locations in part of South Eastern Nigeria. Iraqi Journal of Science, Vol. 60, No. 5, 2019, pp. 1013-1022.

Al-Ani A.A. The optimum investment of groundwater in Fatha-Samarra basin. M.Sc. thesis, college of science, University of Baghdad, 1997, 114 p.

AL-Awsi M.H. and Abdulrazzaq Z.T. Implementing electrical resistivity tomography to delineate soil contamination zone, Southern Baqubah City, Iraq. Kuwait Journal of Science, Vol. 49, No. 2, 2022, https://doi.org/10.48129/kjs.10674.

Al-Janabi M.A.J. Hydrochemistry of the unconfined aquifer and the relationship of unsaturated zone sediments on the groundwater quality in Tikrit – Samara basin, Ph.D. thesis, college of science, University of Baghdad, 2008, 154 p.

Al-Jobori N.H. Hydrogeological conditions of Baiji-Tikrit sub basin, M.Sc. thesis, college of science, University of Tikrit, 2011, 164 p.

Al-Kadhimi J.A.M., Sissakian V.K., Satter A.F., Diekran D.B. Tectonic map of Iraq, Scale 1:1,000,000. 2nd Edition, GEOSURV, Baghdad, 1996.

Al-Minshid F.H.K. Groundwater study of Al-Dhibaee area using electrical survey and pumping test wells. M.Sc. thesis, college of science, University of Baghdad, 2001, 119 p.

Basi M.A. and Karim S.A. The stage report of the local geological survey, Vol. 2, 1990, Laboratory Studies.

Bobachev C. "IPI2Win": a Windows software for an automatic interpretation of resistivity sounding data. PhD tesis, Moscow State University, Moscow, Russia, 2002, 320 p.

Buday T. and Jassim S. Tectonic map of Iraq (A), scale 1:1000000. Iraq Geol. Surv. Publ., Baghdad, 1984.

de Almeida A., Maciel D.F., Sousa K.F., Nascimento C.T.C., Koide S. Vertical electrical sounding (VES) for estimation of hydraulic parameters in the porous aquifer. Water, Vol. 13, No.2, 2021, 170, https://doi.org/10.3390/w13020170.

Gaikwad S., Pawar N.J., Bedse P., Wagh V., Kadam A. Delineation of groundwater potential zones using vertical electrical sounding (VES) in a complex bedrock geological setting of the West Coast of India. Modeling Earth Systems and Environment, 2021, pp. 1-15, https://doi.org/10.1007/ s40808-021-01223-3.

Hamza N.M., Lawa F., Yacoub S.Y., Mussa A.Z., Fouad S.F. Regional geological stage report. SEGESMI, Baghdad. Project C.E.S.A., Geological Activity, No. 2023 of Iraq Geol. Surv. Libr. Rep., 1990.

Jassim S.Z., Goff J. Geology of Iraq. Dolin, Prague and Moravian Museum. Brno, 2006, 341 p.

Keller G.V. Application of resistivity methods in mineral and groundwater exploration program. Mining and Groundwater Geophysics, Geological Survey of Canada, No. 26, 1967, pp. 51-66.

Kosinski W.K., Kelly W.E. Geoelectric soundings for predicting aquifer properties. Groundwater, Vol. 19, 1981, pp. 163-171.

Lech M., Skutnik Z., Bajda M., Markowska-Lech K. Applications of electrical resistivity surveys in solving selected geotechnical and environmental problems. Applied Sciences, Vol. 10, No. 7, 2020, 2263, https://doi.org/10.3390/ app10072263.

Orellana E., Mooney H.M. Master tables and curves for vertical electrical sounding over layered structures. Interciencia. Madrid, Spain, 1966, 34 p.

Oudeika M.S., Taşdelen S., Güngör M., Aydin A. Integrated vertical electrical sounding and hydrogeological approach for detailed groundwater pathways investigation: Gökpınar Dam Lake, Denizli, Turkey. Journal of African Earth Sciences, Vol. 182, 2021, 104273, https://doi.org/10.1016/ j.jafrearsci.2021.104273.

Soomro A., Qureshi A.L., Jamali M.A., Ashraf A. Groundwater investigation through vertical electrical sounding at hilly area from Nooriabad toward Karachi. Acta Geophysica, Vol. 67, No. 1, 2019, pp. 247-261., https://doi.org/10.1007/ s11600-019-00247-9.

Virupaksha H.S., Lokesh K.N. Electrical resistivity, remote sensing and geographic information system approach for mapping groundwater potential zones in coastal aquifers of Gurpur watershed. Geocarto International, Vol. 36, No. 8, 2021, pp. 888-902, https://doi.org/10.1080/10106049.2019. 1624986.

Youssef M.A.S. Geoelectrical analysis for evaluating the aquifer hydraulic characteristics in Ain El-Soukhna area, West Gulf of Suez, Egypt. NRIAG Journal of Astronomy and Geophysics, Vol. 9, No. 1, 2020, pp. 85-98.

Zohdy A.A.R. A new method for the automatic interpretation of Schlumberger and Wenner sounding curves. Geophysics, Vol. 54, No. 2, 1989, pp. 245-253.

Zohdy A.A.R., Bisdorf R.J. Schlumberger soundings near Medicine Lake, California. Geophysics, Vol. 55, No. 8, 1990, pp. 956-964.

Buday T. and Jassim S. Tectonic map of Iraq (A), scale 1:1000000. Iraq Geol. Surv. Publ., Baghdad, 1984.

de Almeida A., Maciel D.F., Sousa K.F., Nascimento C.T.C., Koide S. Vertical electrical sounding (VES) for estimation of hydraulic parameters in the porous aquifer. Water, Vol. 13, No.2, 2021, 170, https://doi.org/10.3390/w13020170

Gaikwad S., Pawar N.J., Bedse P., Wagh V., Kadam A. Delineation of groundwater potential zones using vertical electrical sounding (VES) in a complex bedrock geological setting of the West Coast of India. Modeling Earth Systems and Environment, 2021, pp. 1-15, https://doi.org/10.1007/ s40808-021-01223-3

Hamza N.M., Lawa F., Yacoub S.Y., Mussa A.Z., Fouad S.F. Regional geological stage report. SEGESMI, Baghdad. Project C.E.S.A., Geological Activity, No. 2023 of Iraq Geol. Surv. Libr. Rep., 1990.

Jassim S.Z., Goff J. Geology of Iraq. Dolin, Prague and Moravian Museum. Brno, 2006, 341 p.

Keller G.V. Application of resistivity methods in mineral and groundwater exploration program. Mining and Groundwater Geophysics, Geological Survey of Canada, No. 26, 1967, pp. 51-66.

Kosinski W.K., Kelly W.E. Geoelectric soundings for predicting aquifer properties. Groundwater, Vol. 19, 1981, pp. 163-171.

Lech M., Skutnik Z., Bajda M., Markowska-Lech K. Applications of electrical resistivity surveys in solving selected geotechnical and environmental problems. Applied Sciences, Vol. 10, No. 7, 2020, 2263, https://doi.org/10.3390/ app10072263.

Orellana E., Mooney H.M. Master tables and curves for vertical electrical sounding over layered structures. Interciencia. Madrid, Spain, 1966, 34 p.

Oudeika M.S., Taşdelen S., Güngör M., Aydin A. Integrated vertical electrical sounding and hydrogeological approach for detailed groundwater pathways investigation: Gökpınar Dam Lake, Denizli, Turkey. Journal of African Earth Sciences, Vol. 182, 2021, 104273, https://doi.org/10.1016/ j.jafrearsci.2021.104273.

Soomro A., Qureshi A.L., Jamali M.A., Ashraf A. Groundwater investigation through vertical electrical sounding at hilly area from Nooriabad toward Karachi. Acta Geophysica, Vol. 67, No. 1, 2019, pp. 247-261., https://doi.org/10.1007/ s11600-019-00247-9.

Virupaksha H.S., Lokesh K.N. Electrical resistivity, remote sensing and geographic information system approach for mapping groundwater potential zones in coastal aquifers of Gurpur watershed. Geocarto International, Vol. 36, No. 8, 2021, pp. 888-902, https://doi.org/10.1080/10106049.2019. 1624986.

Youssef M.A.S. Geoelectrical analysis for evaluating the aquifer hydraulic characteristics in Ain El-Soukhna area, West Gulf of Suez, Egypt. NRIAG Journal of Astronomy and Geophysics, Vol. 9, No. 1, 2020, pp. 85-98.

Zohdy A.A.R. A new method for the automatic interpretation of Schlumberger and Wenner sounding curves. Geophysics, Vol. 54, No. 2, 1989, pp. 245-253.

Zohdy A.A.R., Bisdorf R.J. Schlumberger soundings near Medicine Lake, California. Geophysics, Vol. 55, No. 8, 1990, pp. 956-964.

ОЦЕНКА ГИДРОГЕОФИЗИЧЕСКИХ ПАРАМЕТРОВ ПОРИСТОГО ВОДОНОСНОГО ГОРИЗОНТА С ИСПОЛЬЗОВАНИЕМ ГЕОЭЛЕКТРИЧЕСКОЙ МЕТОДИКИ НА ПРИМЕРЕ СУББАССЕЙНА БАЙДЖИ-ТИКРИТ, ИРАК

Абдулраззак З.Т.[1], Ахмед М.М.[2], Салих С.А.[2], Асфагани Дж.[3]

[1]Управление по космосу и связи, Министерство науки и технологий, Багдад, Ирак
10070: zaidoon.taha@live.com
[2]Отдел прикладной геологии, Научный Колледж, Университет Тикрита, Тикрит, Ирак: dr.muhana@tu.edu.iq (M.M.A), sabbar.saleh@tu.edu.iq (S.A.S)
[3]Отдел геологии, Комиссия по атомной энергии, Дамаск, Сирия,
P.O. Box 6091: jasfahani@aec.org.sy

Резюме. Подземные воды являются одним из альтернативных источников воды для компенсации дефицита поверхностных вод, который обычно исследуется геофизическими методами. В суббассейне Байджи-Тикрит, Ирак проведено геоэлектрическое исследование с применением метода вертикального электрического зондирования (VES) для определения мощности, простирания и гидравлических параметров основных водоносных горизонтов. Всего было выполнено 40 измерений ВЭЗ, распределенных вдоль шести геоэлектрических профилей с использованием конфигурации "Шлюмберже" с максимальным половинным интервалом в 400 м (AB/2 = 400 м), где была достигнута глубина проникновения 151 м. Кривые ВЭЗ обработаны и интерпретированы вручную методом вспомогательных точек и автоматически с помощью программного обеспечения IPI2win с использованием ручного инверсного моделирования для уменьшения отношения среднеквадратичных ошибок и повышения точности интерпретации. В результате инверсии было определено, что мощность основного водоносного горизонта составляет 50-128 м. Итоги интерпретации были использованы для построения шести геоэлектрических разрезов вдоль съемочного маршрута. Также было установлено, что основной водоносный горизонт района состоит из осадочных пород (песок, глинистый песок и глина), которые относятся к формации Инджан, и может меняться в районе от ограниченного типа к полуограниченному. Между геоэлектрическими и гидравлическими параметрами были установлены конкретные эмпирические соотношения. Они применяются для расчета гидравлической проводимости (K) и пропускной способности (T) среднего водоносного горизонта в районе исследования. Полученные значения K и T используются для отслеживания их пространственных изменений с целью выделения участков, пригодных для размещения новых скважин.

Ключевые слова: *ВЭЗ, ручное обратное моделирование, гидрогеологические характеристики, пропускная способность, суббассейн Байджи-Тикрит, Ирак*

İRAQ, BAYCİ-TİKRİT SU HÖVZƏSİ TƏDQİQATLARI ÜZRƏ GEOELEKTRİK METODLARDAN İSTİFADƏ ETMƏKLƏ MƏSAMƏLİ SU TƏBƏQƏSİNİN HİDRO-GEOFİZİKİ PARAMETRLƏRİNİN QİYMƏTLƏNDİRİLMƏSİ

Əbdülrəzzaq Z.T.[1], Əhməd M.M.[2], Saleh S.A.[2], Əsfəhani J.[3]
[1]Rabitə və əlaqə idarəsi, Elm və texnologiya nazirliyi, Bağdad, İraq
10070, Iraq: zaidoon.taha@live.com
[2]Tətbiqi geologiya şöbəsi Elmi kollec,Tikrit Universiteti, Tikrit, İraq:
dr.muhana@tu.edu.iq (M.M.A.), sabbar.saleh@tu.edu.iq (S.A.S)
[3]Geologiya şöbəsi, Atom enerjisi üzrə komissiya, Dəməşq, Suriya
P.O.Box 6091: jasfahani@aec.org.sy

Xülasə. Qrunt suları adətən geofiziki üsullarla tədqiq olunan, səthdəki su çatışmazlığını kompensasiya edən alternativ su mənbələrindən biridir. Əsas su təbəqələrinin qalınlığını, uzunluğunu və hidravlik parametrlərini təyin etmək üçün şaquli elektrik zondunu tətbiq etməklə, Bayci-Tikrit yarımhövzəsində İraqda geoelektrik tədqiqatı həyata keçirilir. Şlümberq konfiqurasiyasından istifadə etməklə, dərinliyi 151 metrə çatmaqla, maksimal 400 metr yarim intervalda (AB/2=400 m) altı geoelektrik profilə üzrə paylanmış ümumilikdə qırx ŞEZ yerinə yetirilib. Orta kvadratlı xəta əmsalını azaltmaq və interpretasiya dəqiqliyini artırmaq məqsədilə inversiya modelləşməsindən istifadə etməklə əlilə köməkçi nöqtə metodu və avtomatik olaraq İPİ2 proqramlari vasitəsilə ŞEZ əyriləri emal edilmişdir.

İnversiya nəticələri göstərdi ki, əsas su təbəqəsinin qalınlığı təxminən 50-128 metrdir. Müşahidə keçidləri boyunca altı geoelektrik kəsilişi çəkmək məqsədilə interpretasiya nəticələrindən istifadə olunub. Bu nəticələr göstərdi ki ərazinin əsas su təbəqəsi məhdud növdən yarıməhdud növə keçməyə uygun olan İncana formasiyasına məxsus çöküntülərdən (qum gilli qum və qum) ibarətdir. Geoelektrik və hidravlik parametrlər arasında spesifik empirik (təcrübi) əlaqələrin əsası qoyulub. Onlardan tədqiq olunan ərazidə əsas su təbəqəsinin hidravlik keçiriciliyini (K) və ötürücülüyünü hesablamaq məqsədilə istifadə olunub. K və T dəyərlərinin nəticələrindən yeni quyuların yerləri üçün uygun əraziləri müəyyənləşdirməklə məkan dəyişkənliklərini izləmək məqsədilə istifadə olunub.

Açar sözlər: *ŞEZ, əks modellik, hidro-geoloji xarakteristika, ötürücülük, Bayci-Tikrit yarımhövzəsi, İraq*